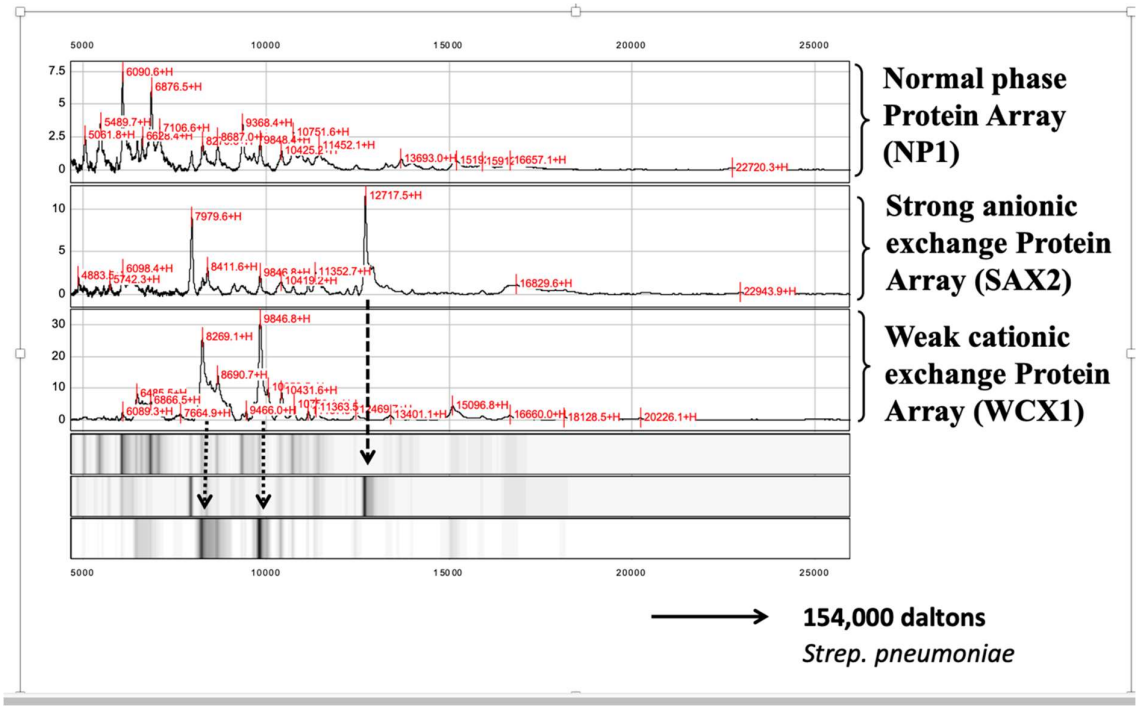

Figure 10.1. MALDI-TOF MS profiles obtained for the same sample using three different ProteinChip arrays (NP1, SAX2 and WCX1) to reveal the complexity of a sample. To enable rapid visual comparison of spectra, the software converted the mass ions into a Gel view images; the greater the mass intensity, the darker the band. (Adapted from Shah *et al.,* 2010, Changing concepts in the characterisation of microbes and the influence of mass spectrometry. In: Shah H.N. and Gharbia, S.E. (eds). '*Mass Spectrometry for Microbial Proteomics'* Wiley, Chichester, pp. 3- 34.

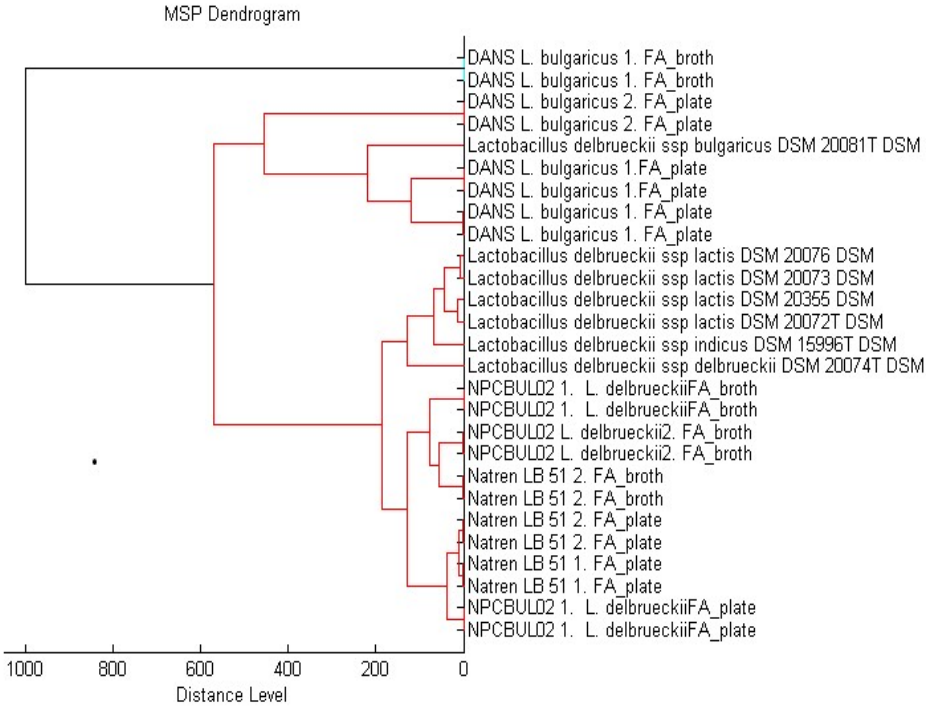

Figure 10.2. The separation of *Lactobacillus* species and subspecies using Bruker Biotyper (software version 3.0). The results highlight the capacity of MALDI-TOF MS to delineate some taxa to the subspecies level. These include: *Lactobacillus delbrueckii* subspecies *delbrueckii, Lactobacillus delbrueckii* subspecies *lactis* and *Lactobacillus delbrueckii* subspecies *indicus* which are frequently used by various probiotic companies.

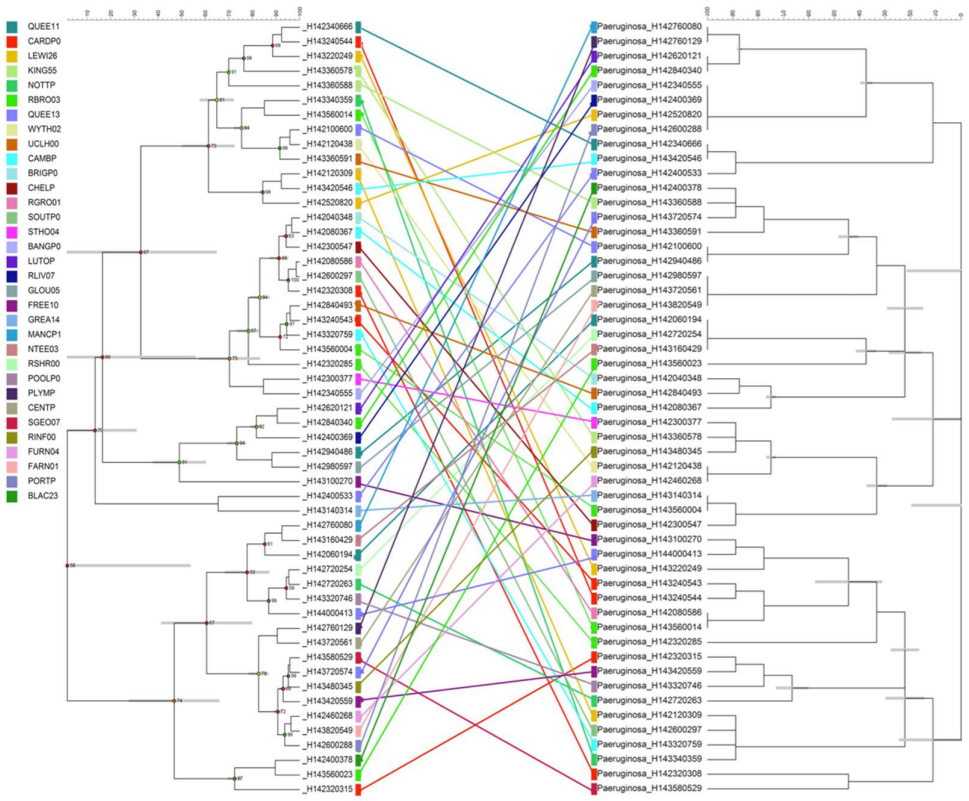

Figure 10.3. Dendrograms showing phenotypic similarities and relationships of 53 *Pseudomonas aeruginosa* strains from cystic fibrosis (CF) and non-CF sites and the same strains analyzed genetically using VNTR (variable number tandem repeat). Congruence between the phylotypes was negligible and indicate that one method cannot supplant another. (Adapted from Olkun, Shah and Shah, 2017, 'Elucidating the intraspecies proteotypes of *Pseudomonas aeruginosa* from cystic fibrosis. In: Shah, H.N. and Gharbia, S.E. (eds). *MALDI-TOF and Tandem MS for Clinical Microbiology*. Wiley, Chichester, UK, pp 579 - 592.

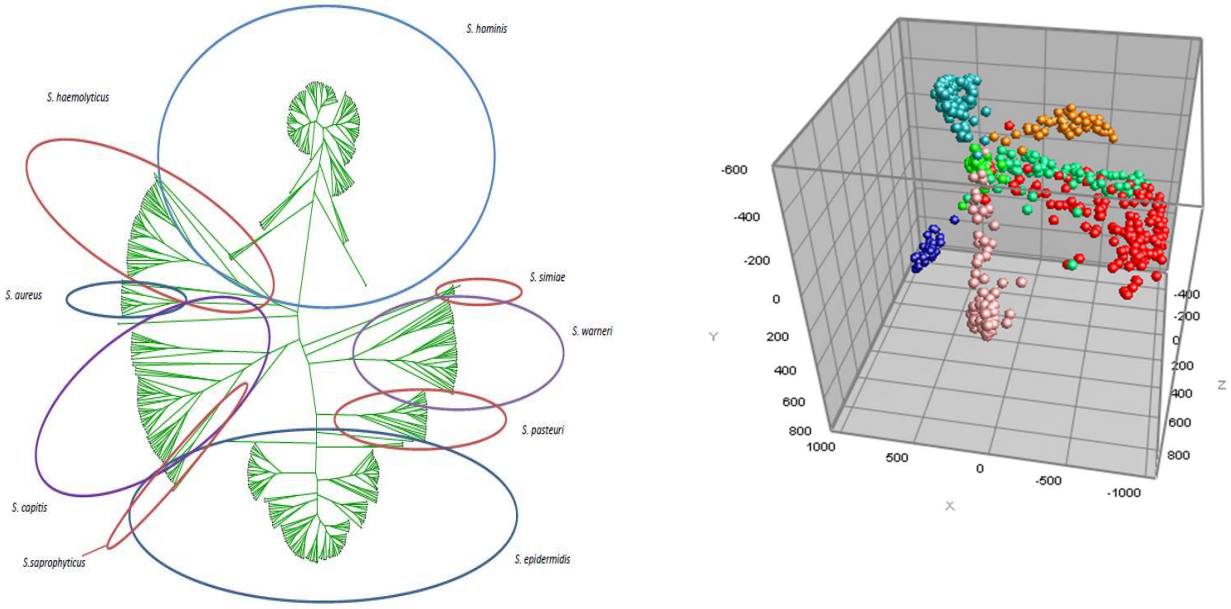

Figure 10.4 (Left) Unrooted cluster analysis of staphylococcus species in the community based upon MALDI-TOF MS spectral profiles. While each species was distinctively delineated, the data enabled the intraspecies diversity to be clearly discerned (Xu *et. al,* 2017. Adapted from "Subtyping of *Staphylococcus* spp. based upon MALDI-TOF MS data analysis. In: Shah, H.N. and Gharbia, S.E. (eds). *MALDI-TOF and Tandem MS for Clinical Microbiology*. Wiley, Chichester, UK, pp 563 - 378.

(Figure 10.4 (Right) Three-dimensional scatter plot *Staphylococcus aureus* isolates using a supervised method such as linear discriminant analysis (LDA, Bionumerics) to show relationships among isolates from specific sites which may be useful for identifying unique traits during transmission (Adapted from Vranckx, K., De Bruyne, K. and Pot, B. (2017) "Analysis of MALDI-TOF MS spectra using the BioNumerics software". In: Shah, H.N. and Gharbia, S.E. (eds). MALDI-TOF and Tandem MS for Clinical Microbiology. Wiley, Chichester, UK, pp 539-562.

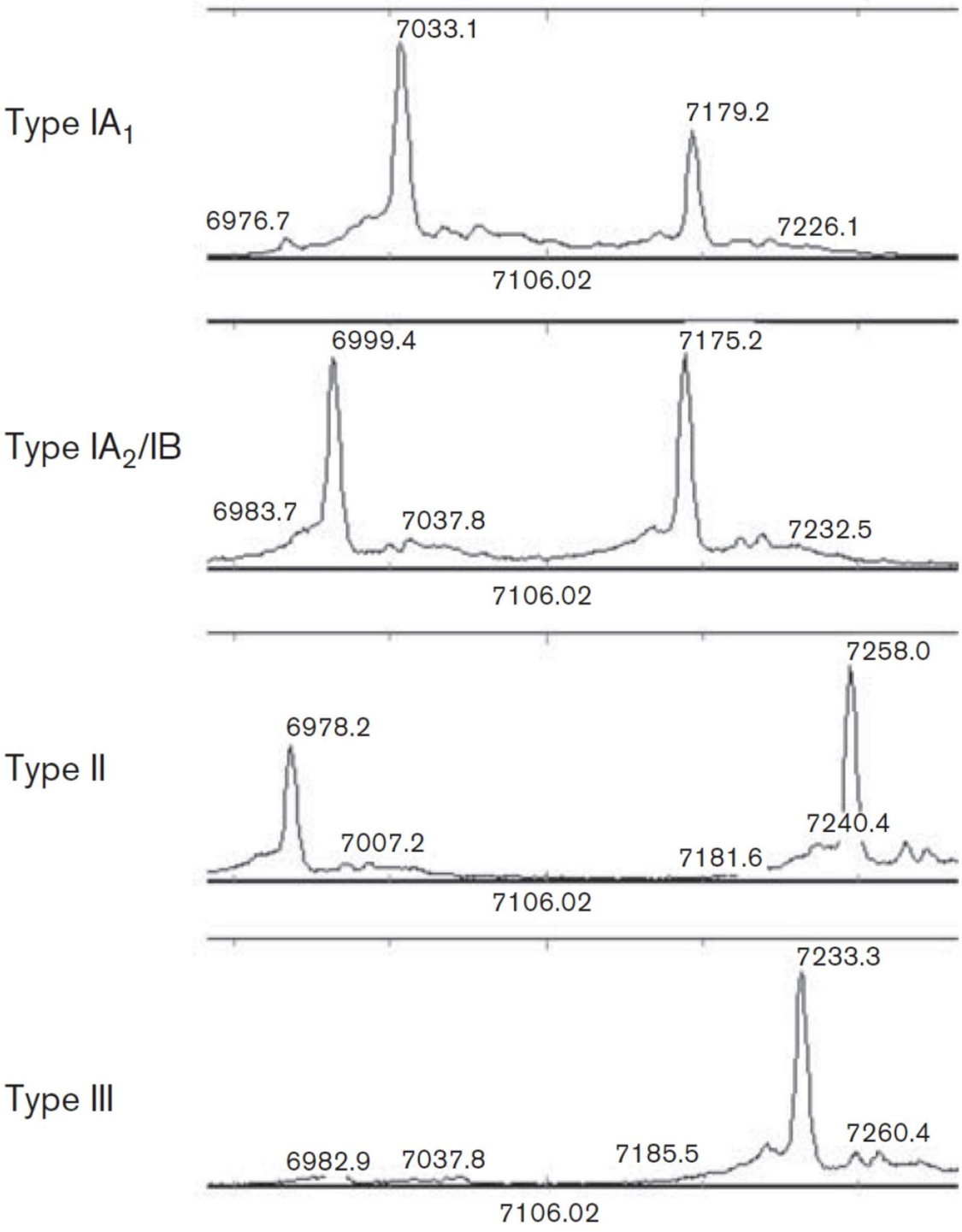

Figure 10.5. Unique biomarker mass ions in the MALDI-TOF MS spectrum of *Cutibacterium acnes* subspecies (Dekio *et al*. 2015).

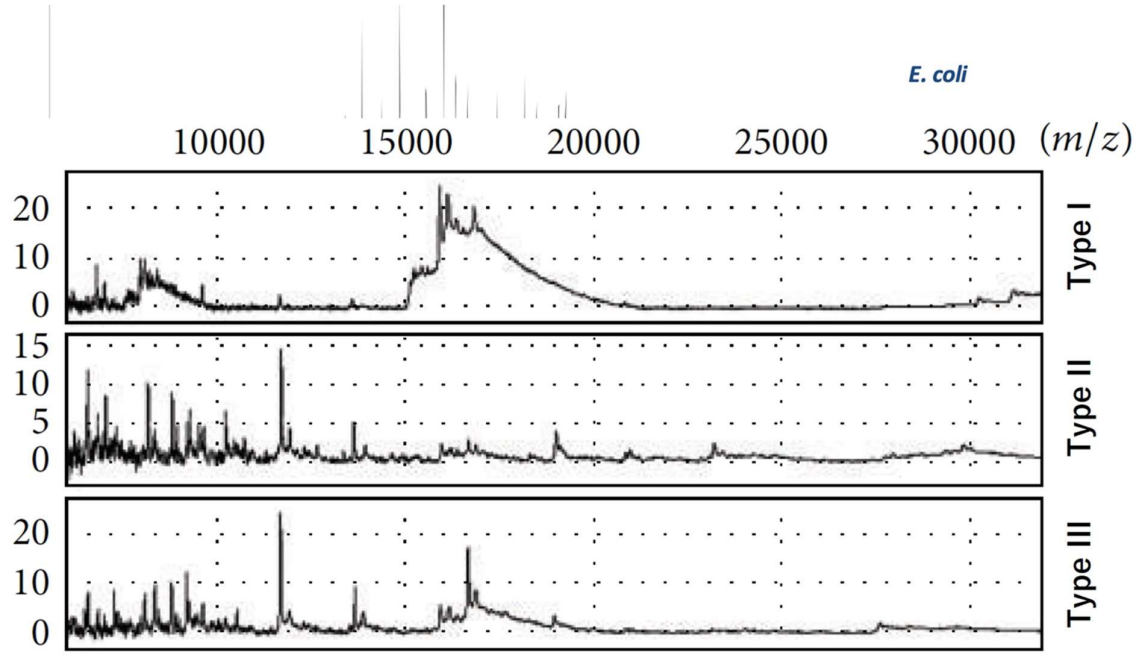

Figure 10.6. Unique biomarker mass ions between 10-20 kD segment of the SELDI-TOF MS spectra of anaerobically-cultured *Cutibacterium acnes* isolates.

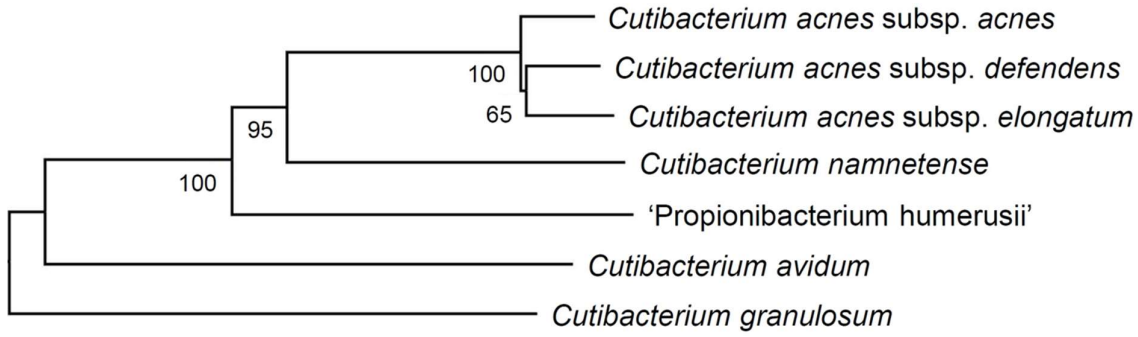

Figure 10.7. Genome phylogram for type strains of *Cutibacterium* species and subspecies that confirmed the initial data obtained by MALDI-TOF and SELDI-TOF MS analyses and emphasise the value of the latter techniques in preliminary screening of isolates from diverse habitats.

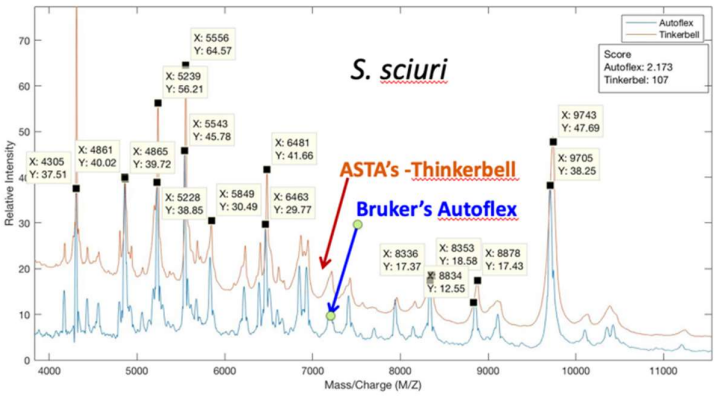

ID	Species	Bruker species	Bruker score	ASTA species	ASTA score
211	*S. cohnii*	Not reliable ID	1.657	Invalid ID	96
		S. capitis	1.725	Invalid ID	90
		S. cohnii	1.874	Invalid ID	89
295	*S. cohnii*	Not reliable id	1.665	*S. cohnii*	223
		Not reliable id	1.445	*S. cohnii*	152
		S. cohnii	1.771	*S. cohnii*	207
297	*S. cohnii*	*S. cohnii*	1.703	*S. cohnii*	235
		S. cohnii	1.965	*S. cohnii*	237
		S. cohnii	1.827	*S. cohnii*	235
319	*S. cohnii*	*S. cohnii*	1.846	*M. lylae*	180
		S. cohnii	1.832	*M. lylae*	168
		S. cohnii	1.834	*M. lylae*	165
342	*S. cohnii*	*S. cohnii*	1.816	*S. cohnii*	239
		S. cohnii	1.766	*S. cohnii*	249
		S. cohnii	1.884	*S. cohnii*	252
343	*S. cohnii*	*S. cohnii*	1.848	*S. cohnii*	228
		S. cohnii	1.993	*S. cohnii*	219
		S. cohnii	1.927	*S. cohnii*	227
344	*S. cohnii*	*S. cohnii*	1.856	*S. cohnii*	230
		S. cohnii	1.933	*S. cohnii*	221
		S. cohnii	1.866	*S. cohnii*	217
345	*S. cohnii*	*S. cohnii*	1.821	*S. cohnii*	219
		S. cohnii	1.904	*S. cohnii*	222
		S. cohnii	1.702	*S. cohnii*	216
347	*S. cohnii*	*S. cohnii*	1.702	*S. cohnii*	221
		S. cohnii	2.026	*S. cohnii*	231
		Not reliable id	1.648	*S. cohnii*	222
349	*S. cohnii*	*S. cohnii*	1.807	*S. cohnii*	222
		S. cohnii	1.991	*S. cohnii*	236
		S. cohnii	1.955	*S. cohnii*	239

Figure 10.8. (Left). MALDI-TOF MS analysis of staphylococcal species using ASTA's Tinkerbell Linear MS and Bruker's Autoflex LRF MALDI TOF MS. An example using *Staphylococcus sciuri* showing the spectrum obtained on ASTA's Tinkerbell Linear MS (red) which was superimposed on the Bruker's Autoflex LRF MALDI TOF MS spectrum (light blue). The results show unequivocally the correspondence of the major mass ions of this species.
Figure 10.8 (Right). 16S rRNA identification of 10 atypical strains of *Staphylococcus cohnii.* Both instruments revealed low identification scores, but most samples were correctly identified. The identification scores of seven strains were too low to provide an identification while strain 319 was incorrectly identified as *Mycobacterium lylae* using ASTA's Tinkerbell MS. Once added to the ASTA database, this and other strains were correctly identified.

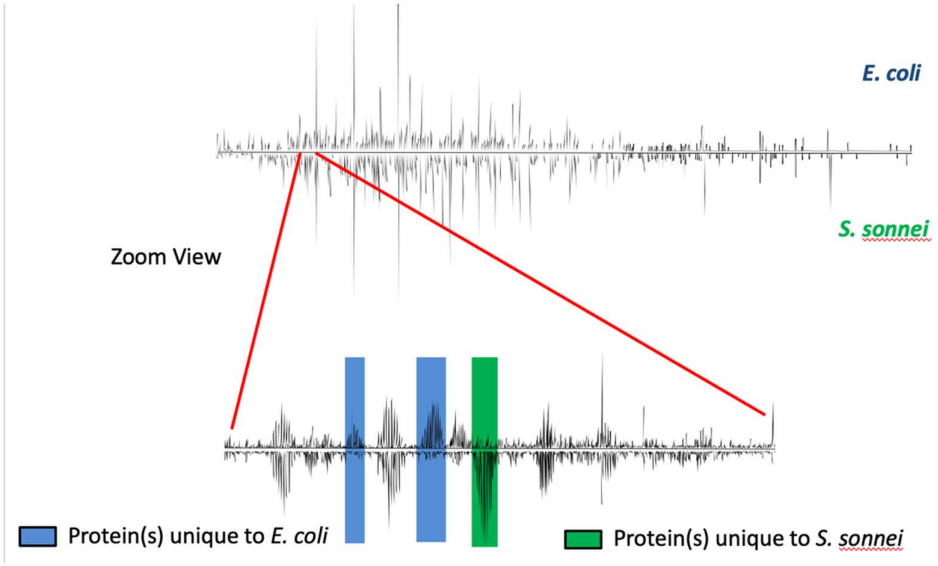

Figure 10.9. Use of Top-Down Proteomics to delineate genetically closely related species. In an early attempt to demonstrate the high resolution of this approach, proteins unique to both species were evident but were differentially expressed (Shah *et. al.,* 2015).